WATER RESOURCES RESEARCH, VOL. 29, NO. 6, PAGES 1621–1633, JUNE 1993

Multiporosity/Multipermeability Approach to the Simulation of Naturally Fractured Reservoirs

MAO BAI[1]

School of Petroleum and Geological Engineering, University of Oklahoma, Norman

DEREK ELSWORTH

Department of Mineral Engineering, Pennsylvania State University, University Park

JEAN-CLAUDE ROEGIERS

School of Petroleum and Geological Engineering, University of Oklahoma, Norman

This paper presents an array of deformation-dependent flow models of various porosities and permeabilities relevant to the characterization of naturally fractured reservoirs. A unified multiporosity multipermeability formulation is proposed as a generalization of the porosity- or permeability-oriented models of specific degree. Some new relationships are identified in the parametric investigation for both single-porosity and dual-porosity models. A formula is derived to express Skempton's constant B by Biot's coefficient H and relative compressibility ϕ^*. It is found that the recovery of the original expression for Skempton's constant B is largely dependent on the choice of ϕ^*, representing relative compressibility. The dual-porosity/dual-permeability model is evaluated through an alternative finite element approximation. The deformation-dependent fracture flow mechanism is introduced where the rock matrix possesses low permeability and fracture flow is dominant. A preliminary study of the reservoir simulation identifies the strong coupling between the fluid flow and solid deformation.

1. INTRODUCTION

Fractured rock may be considered as a multiporous medium [*Aifantis*, 1980] where fractures and intervening porous blocks are the most obvious components of the dual-porosity system. In a typical fractured reservoir, fractures provide high-conductivity conduits amenable to rapid hydraulic flows, whereas the high-porosity matrix blocks contain the majority of the storage. Therefore the behavior of naturally fractured reservoirs is radically different from that of a conventional reservoir composed solely of intergranular porosity and permeability.

Theoretical study of the dual-porosity system was initiated by *Barenblatt et al.* [1960] by introducing the theory of mixtures. In their model, the fractured medium is represented by two completely overlapping continua, one representing the porous matrix and the other representing the fractures (Figure 1). The dual-porosity model proposed by Barenblatt et al. was further modified by *Warren and Root* [1963] to represent the naturally fractured reservoir as an idealized system formed by identical rectangular parallelepipeds, separated by an orthogonally fractured network.

For the purpose of accurately characterizing the pressure buildup or depletion history of reservoirs, considerable interest has been focused on developing realistic mechanisms depicting the interporosity flow in naturally fractured reservoirs. The focal point is to fit the transient transition curve where the important fluid interchange between fractures and matrix blocks occurs. In general, interporosity flow has been described by two mechanisms. The first is the simple quasi-steady state model proposed by *Warren and Root* [1963], followed by the more sophisticated unsteady state models of various versions [*Kazemi*, 1969; *deSwaan-O.*, 1976; *Duguid and Lee*, 1977; *Kucuk and Sawyer*, 1980; *Najurieta*, 1980; *Chen et al.*, 1985]. Some noticeable differences in terms of pressure distributions in the transition period result from the two different mechanisms.

The transient flow and deformation behavior in a porous medium may result from changes in either the fluid pressure or total stress boundary conditions applied to the system. It is the admissibility of changes in total stress within the system (which may result from natural tectonic changes or human activities) that describes the essence of coupled deformation-dependent flow behavior within porous media and sets it apart from decoupled diffusive (flow) systems. Comprehensive coupling between stresses and pore pressures was first rationalized by *Biot* [1941] and later adopted in many applications to specific deformation flow systems [*Ghaboussi and Wilson*, 1973; *Zienkiewicz et al.*, 1977; *Simon et al.*, 1984; *Lewis and Schrefler*, 1987; *Detournay and Cheng*, 1988]. In naturally fractured reservoirs where the medium consists of discrete fractions of varying solid compressibilities and permeabilities, a multiporosity/multipermeability approach appears more appropriate.

It is important to correctly characterize the behavior of naturally fractured reservoirs. For example, the exceptionally high oil rate recovered in the initial stages of reservoir production may lead to overestimating well production by assuming a higher storage to exist than exists in reality. It was assumed that the high matrix block storage would

[1]Formerly at J. F. T. Agapito and Associates, Inc., Grand Junction, Colorado.

Paper number 92WR02746.
0043-1397/93/92WR-02746$05.00

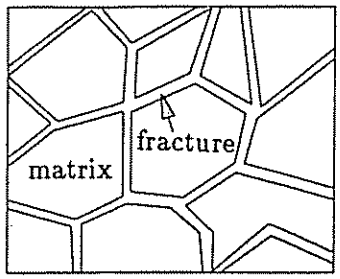

Fig. 1. Fractured reservoir rock.

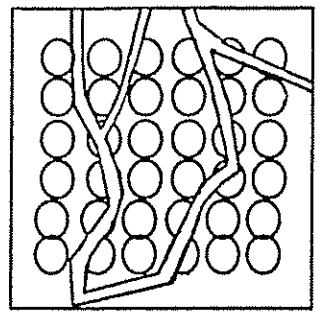
Fig. 3. Reservoir with large storage in matrix.

continuously render the supply to the well through highly permeable fracture channels. In fact, many reservoirs that produce at high initial rates decline drastically after a short period of time because the oil has been stored in the fracture system (Figure 2). As *Aguilera* [1980] pointed out, it is important to visualize that the storage capacity of naturally fractured reservoirs varies extensively, depending on the degree of fracturing in the formation and the value of the primary porosity. In contrast to this scenario, Figure 3 illustrates a case where only a small percentage of the total porosity is resident in the fractures. Averaging from the two extremes, an ideal situation for oil production is depicted in Figure 4 where about equal storage capacity exists in the fractures and matrix blocks. In summary, it is not safe to say that the storage capacity of a fractured system is negligible compared to the storage of the matrix.

Another important parameter for production is permeability, a measure of the capacity of the medium to transmit fluid which has a dimension of area. In general, fractures possess substantially higher permeability than that of the matrix itself, which is a crucial factor in a tight reservoir where economical production is desired. However, the porous media essentially collapse to be of an equivalent single permeability for a healed fracture system.

The critical impact of strata deformation such as reservoir compaction in changing flow systems has been recognized in many circumstances. A typical example is the surface subsidence as a result of groundwater pumping or petroleum production. Accurate prediction of subsidence and fluid pressure control can be enhanced through using a deformation-dependent flow model coupled with a proper validation via field measurement.

To provide the industry with more flexible tools in matching the geological variations and to avoid an unrealistic prediction of reservoir storage locations which may lead to production failure, several conceptual deformation-dependent flow models are proposed in the following. These are presented together with their respective governing equations based on a generalized multiporosity/multipermeability principle. Following a discussion on parametric determination, the formulation of the deformation-dependent flow system is focused on a dual-porosity/dual-permeability scenario which appears to represent one of the traditional types of naturally fractured reservoirs in view of petroleum production. The important deformation effect on the fluid pressure distribution is identified in two hypothetical case studies.

2. Conceptual Models of Various Porosities and Permeabilities

In the following, an array of deformation-dependent flow models is either rewritten (models 1 and 3) or proposed (models 2, 4, and 5) in concise tensor forms. In addition, a general multiporosity/multipermeability formulation is given based on mixture theory.

2.1. *Model 1: Single-Porosity/Single-Permeability*

The study of fluid flow in deformable, saturated porous media as a coupled deformation-dependent flow system was initiated with the work of *Terzaghi* [1943] in his one-dimensional consolidation model. The Terzaghi theory was a special case of a more general three-dimensional form by *Biot* [1941]. In all the development that follows, the porous medium is assumed to possess a continuous distribution of a single type of void space satisfying a single permeability (as shown in Figure 5), which may be termed as a single-porosity/single-permeability medium.

The general stress-strain relationship incorporating effective stress effects through pore pressures may be written as

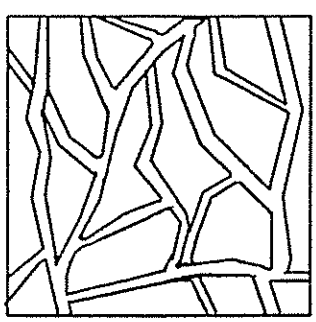
Fig. 2. Reservoir with all storage in fractures.

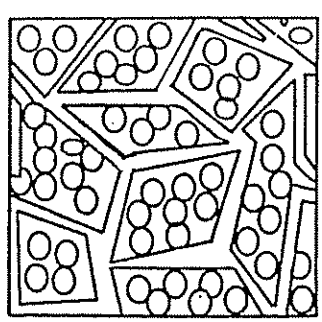
Fig. 4. Reservoir with equal storage.

$$\varepsilon_{ij} = \frac{1+\nu}{E}\sigma_{ij} - \frac{\nu}{E}\sigma_{kk}\delta_{ij} - \frac{\phi}{3H}p\delta_{ij}, \quad (1)$$

where E is the elastic modulus, ν is the Poisson ratio, ϕ is the pressure ratio factor, H is the Biot constant, σ_{kk} is total stress, p is fluid pressure, δ_{ij} is the Kronecker delta, and ε_{ij} and σ_{ij} are strain and stress tensors, respectively. In this analysis, the Greek and Latin subscripts have the values of 1, 2 and 1, 2, 3, respectively; a comma stands for differentiation and summation is implied over the repeated Latin subscripts.

The equilibrium equation in the absence of self weight and inertial effects may be given as

$$\sigma_{ij,j} = 0 \quad (2)$$

and the strain–displacement relation is defined as

$$\varepsilon_{ij} = \tfrac{1}{2}(u_{i,j} + u_{j,i}), \quad (3)$$

where u_i are displacements. The equation governing a solid body deformation is obtained through substitution of (1) and the strain-displacement relation of (3) into the equilibrium equation (2), to yield

$$Gu_{i,jj} + (\lambda + G)u_{k,ki} + \phi p_{,i} = 0, \quad (4)$$

where G is the shear modulus and λ is a Lamé constant.

In the fluid phase, Darcy flow velocity, v_i, can be expressed as

$$v_i = -\frac{k}{\mu}p_{,i}, \quad (5)$$

where k is permeability and μ is fluid dynamic viscosity. The basic statement of flow continuity requires that the divergence of the flow velocity be equal to the rate of fluid accumulation per unit volume of space; therefore

$$v_{i,i} = \phi\dot{\varepsilon}_{kk} - \phi^*\dot{p}, \quad (6)$$

where ϕ^* is termed the relative compressibility. Substituting (5) into (6) gives the governing flow equation as

$$-\frac{1}{\mu}kp_{,kk} = \phi\dot{\varepsilon}_{kk} - \phi^*\dot{p}. \quad (7)$$

Equations (4) and (7) constitute the governing equations for the deformation-dependent behavior of a single-porosity/single-permeability medium. In general, this model is applied to a nonfractured reservoir with uniform porosity and permeability.

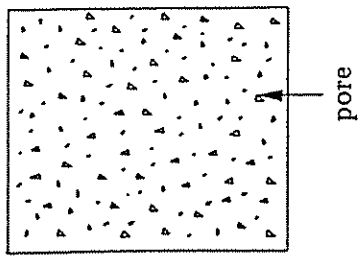

Fig. 5. Single-porosity/single-permeability system.

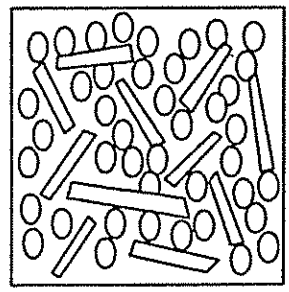

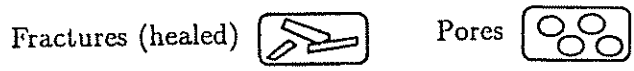

Fig. 6. Dual-porosity/single-permeability system.

2.2. *Model 2: Dual-Porosity/Single-Permeability*

For a fractured medium, it is generally recognized the fractures add secondary porosity to the original porosity by breaking the porous medium into blocks. The dual-porosity conceptualization of a fractured medium considers the fluid in fractures and the fluid in matrix blocks as separate and overlapping continua. However, unlike the common assumption for a dual-porosity medium where the fluid flows primarily through highly permeable fractures, the nonpercolating fractured system depicted in Figure 6 suggests an equivalent single-permeability behavior in a medium with distinctly different porosities. A fractured reservoir with relatively low permeability but high storage (tight reservoir) may be characterized by this dual-porosity/single-permeability model. The governing equation of solid deformation may be expressed as follows:

$$Gu_{i,jj} + (\lambda + G)u_{k,ki} + \sum_{m=1}^{2}\phi_m p_{m,i} = 0, \quad (8)$$

where $m = 1$ and 2 represent fractures and matrix blocks, respectively.

The governing equation for the fluid phase is

$$-\frac{1}{\mu}kp_{m,kk} = \phi_m\dot{\varepsilon}_{kk} - \phi^*_m\dot{p}_m \pm \xi(\Delta p), \quad (9)$$

where k is the equivalent single permeability, or a permeability averaged from the total system, and ξ corresponds to a fluid transfer rate representing the intensity of flow between the fractures and matrix driven by the pressure gradient, Δp. A positive sign indicates outflow from the matrix, and a negative sign indicates inflow into the matrix.

The major difference between the dual-porosity/single-permeability system and the previous single-porosity/single-permeability system is that interporosity flow is permitted in the former. Furthermore, no distinction between fracture permeability and matrix permeability may be identified in the dual-porosity/single-permeability system, which distinguishes it from the conventional dual-porosity/dual-permeability system.

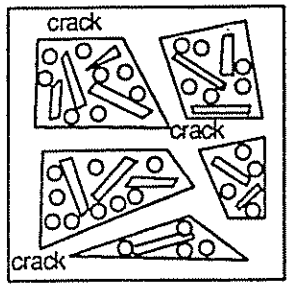

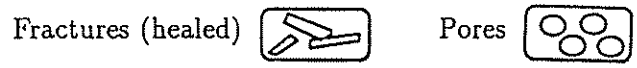

Fig. 7. Triple-porosity/dual-permeability system.

2.3. *Model 3: Dual-Porosity/Dual-Permeability*

This is a commonly accepted naturally fractured reservoir model in which the fracture and matrix phases are distinctly different in both porosity and permeability. In formal language, these media possess two degrees of porosity and permeability. The model may be best represented by Figure 3 where high porosity/low permeability matrix and low porosity/high permeability fractures are typical characteristics of the medium.

In view of the governing equations, the model carries an identical form in the solid phase as the dual-porosity/single-permeability model (equation (8)). However, the equation for the fluid phase differs:

$$-\frac{1}{\mu} k_m p_{m,kk} = \phi_m \dot{\epsilon}_{kk} - \phi^*_m \dot{p}_m \pm \xi(\Delta p), \qquad (10)$$

where k_m is the permeability of phase m.

Under the assumption of low matrix permeability, a fracture flow mechanism may be incorporated in the formulation. The dual-porosity/dual-permeability model is suitable for the simulation of a fractured reservoir with low-permeability matrix blocks.

2.4. *Model 4: Triple-Porosity/Dual-Permeability*

For a severely fractured reservoir, however, a dual-porosity model may not be appropriate even in the local geometry. An immediate extension of the dual-porosity conceptualization is to triple porosity. An example of a triple-porosity model is where a dominant fracture system intercepts a less pervasive and nested fracture system, which in turn is set within a porous matrix.

The term "triple porosity" is not new in the literature. *Abdassah and Ershaghi* [1986] considered a reservoir where fractures have homogeneous properties throughout and interact with two groups of separate matrix blocks that have different permeabilities and porosities. It should be pointed out, however, that the Abdassah and Ershaghi approach could still be considered as a dual-porosity approach, particularly with a numerical technique by which local parametric adjustment may be easily achieved.

In this paper, a truly triple-porosity system or matrix-fissure-crack system is proposed. For a triple-porosity/ dual-permeability system, matrix pores are interwoven with non-percolating fissures, and they interact with open cracks through fluid exchange among different phases (Figure 7). The governing equation for the solid phase is given by

$$G u_{i,jj} + (\lambda + G) u_{k,ki} + \sum_{m=1}^{3} \phi_m p_{m,i} = 0, \qquad (11)$$

where $m = 1$, 2, and 3 are the subscripts for cracks, fissures and matrix, respectively.

For the fluid phase, it is convenient to write out each equation and the corresponding subscript separately, such as

$$-\frac{1}{\mu} k_1 p_{1,kk} = \phi_1 \dot{\epsilon}_{kk} - \phi^*_1 \dot{p}_1 \pm \xi_{12}(p_2 - p_1) \pm \xi_{13}(p_3 - p_1), \qquad (12)$$

$$-\frac{1}{\mu} k_{23} p_{2,kk} = \phi_2 \dot{\epsilon}_{kk} - \phi^*_2 \dot{p}_2 \pm \xi_{21}(p_1 - p_2) \pm \xi_{23}(p_3 - p_2), \qquad (13)$$

$$-\frac{1}{\mu} k_{23} p_{3,kk} = \phi_3 \dot{\epsilon}_{kk} - \phi^*_3 \dot{p}_3 \pm \xi_{31}(p_1 - p_3) \pm \xi_{32}(p_2 - p_3), \qquad (14)$$

where k_1 is the crack permeability, k_{23} is the averaged permeability between the matrix and fissures, and ξ_{ij} is the fluid transfer rate between phase i and phase j. The interporosity flow that results from pressure differentiation is assumed between all three phases.

A severely fractured reservoir with moderate permeability may be represented by a triple-porosity/dual-permeability model.

2.5. *Model 5: Triple-Porosity/Triple-Permeability*

For a percolating fissure system, the permeability is independent for each phase, similar to porosity (Figure 8). The governing equations for the solid phase are identical to (11). For the fluid phase, the change is made solely in the permeability terms. Instead of using the averaged permeability for the matrix and fissures, each phase i carries its respective permeability $k_i (i = 1, 2, 3)$.

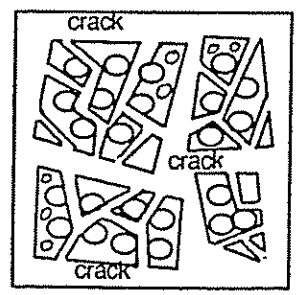

Fig. 8. Triple-porosity/triple-permeability system.

The triple-porosity/triple-permeability model is applicable to a severely fractured reservoir with high permeability.

2.6. *Multiporosity/Multipermeability Model*

By the definition of Aifantis's multiporosity theory [*Aifantis*, 1977, 1980], any media that exhibit finite discontinuities in the porosity field are considered to possess a multiporosity property. However, no unified formulation based on the multiporosity theory has ever been written. Following the previous derivation, the formulation for a multiporosity/multipermeability system is readily available.

In the solid phase, the effect of fluid pressure on the solid deformation within each individual component may be superposed to form

$$Gu_{i,jj} + (\lambda + G)u_{k,ki} + \sum_{m=1}^{I} \phi_m p_{m,i} = 0, \qquad (15)$$

where I is the number of distinct porosities of the porous medium.

In the fluid phase, a separate equation must be written for each component of distinct porosity or permeability. For component 1,

$$-\frac{1}{\mu} k_1 p_{1,kk} = \phi_1 \dot{\varepsilon}_{kk} - \phi_1^* \dot{p}_1 \pm \sum_{i=2}^{I} \xi_{1(i)}(p_i - p_1). \qquad (16)$$

For component j,

$$-\frac{1}{\mu} k_j p_{j,kk} = \phi_j \dot{\varepsilon}_{kk} - \phi_j^* \dot{p}_j \pm \sum_{i=1(j\neq i)}^{I} \xi_{j(i)}(p_i - p_j). \qquad (17)$$

It may be readily demonstrated that the aforementioned single-porosity, dual-porosity, and triple-porosity models are special cases of the unified multiporosity/multipermeability formulation expressed by (15), (16), and (17).

3. PARAMETRIC STUDY

A parametric study is important to illustrate the utility of the multiporosity models identified in section 2. For convenience, the discussion is focused on the study of single-porosity and dual-porosity systems.

3.1. *Single-Porosity Model*

In general, *Terzaghi*'s [1943] effective stress law is defined as

$$\sigma_{ij}^e = \sigma_{ij}^c - p\delta_{ij}, \qquad (18)$$

where σ_{ij}^e is the effective stress tensor and σ_{ij}^c is the total stress tensor. The two important parameters of ϕ in (4) and ϕ^* in (7) require definition. However, the validity of Terzaghi's effective stress remains questionable, in particular for rock engineering, because primary assumptions are of incompressible fluid and grains. Where grain compressibility is finite, a stress ratio term must be added.

In *Biot*'s [1941] theory, the volumetric strain can be written as

$$\theta = \frac{1}{K}\left[\frac{1}{3}\,\mathrm{Tr}\,(\sigma_{ij}) - \frac{K}{H}p\right], \qquad (19)$$

where K is the effective modulus of the skeleton. For isotropic stress conditions, $\theta = (1/K)\sigma^e$, where effective stress σ^e may be redefined as $\sigma^e = (1/3)\sigma_{kk} - \phi p$, where ϕ is termed the pressure ratio factor and σ_{kk} is the total stress. This equation reduces to Terzaghi's theory only when ϕ is unity. Although ϕ may approach unity for compressible rocks [*Kranz et al.*, 1979; *Walsh*, 1981], the magnitude may be determined from both the degree of rock fracturing and solid bulk modulus. *Geertsma* [1957] and *Skempton* [1960] proposed, on experimental grounds, that

$$\phi = 1 - \frac{K}{K_s}, \qquad (20)$$

where K_s is the bulk modulus of grains. *Nur and Byerlee* [1971] verified this relationship theoretically. It is only when the effective compressibility of the dry aggregate is much greater than the intrinsic compressibility of the solid grains ($K \ll K_s$) that the Terzaghi relationship of equation (18) is valid.

In *Biot*'s [1941] approach,

$$\phi = \frac{2(1+\nu)}{3(1-2\nu)}\frac{G}{H} = \frac{E}{3(1-2\nu)H} = \frac{K}{H}, \qquad (21)$$

where H is Biot's constant and can be expressed as

$$\frac{1}{H} = \frac{1}{K} - \frac{1}{K_s}. \qquad (22)$$

It may be noted that only when $K \ll K_s$, $K \approx H$, which is often the case for soil, that Terzaghi's effective stress law holds.

It is a more controversial issue to define the parameter ϕ^*. In a major part, this results from the dispute with regard to the exact form of Terzaghi effective stress law. In Biot's [1941] approach,

$$\phi^* = \frac{1}{R} - \frac{\phi}{H}, \qquad (23)$$

where R is another Biot constant. If Terzaghi's effectiveness stress law is followed, ϕ^* is most widely suggested to be [*Verruijt*, 1969; *Bear*, 1972; *Huyakorn and Pinder*, 1983]

$$\phi^* = \frac{n}{K_f}, \qquad (24)$$

where n is the porosity and K_f is the fluid bulk modulus.

If the compressibility of the solid grains is not negligible, however, then [*Liggett and Liu*, 1983]

$$\phi^* = \frac{n}{K_f} + \frac{1-n}{K_s}. \qquad (25)$$

If we equate (23) and (25) and also note (21) and (22), then R may be derived for Biot's theory as follows:

$$\frac{1}{R} = \frac{n}{K_f} + \frac{1-n}{K_s} + \frac{1}{K}\left(1 - \frac{K}{K_s}\right)^2. \qquad (26)$$

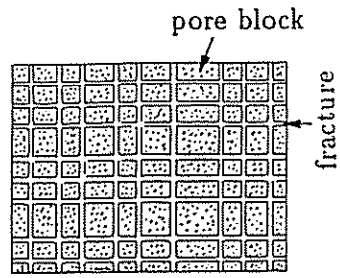

Fig. 9. Dual-porosity fractured medium.

3.2. *Dual-Porosity Model*

The main characteristic of the dual-porosity model is to distinguish between the fracture and intergranular flows. In the general formulation of the dual-porosity model given previously, the possibility exists for flow through both the blocks and the fractures with a transfer function describing the fluid exchange between the two continua.

The important parameters in the governing equations (8) and (10) are ϕ_m, ϕ_m^*, k_m and ξ. It is of interest to rationalize these parameters on certain mechanical grounds.

Due to its equivalence with the pore pressure ratio factor ϕ [*Nur and Byerlee*, 1971], the fluid pressure ratio ϕ_2 in the matrix can be evaluated by (20).

Determination of the fracture fluid pressure ratio ϕ_1 appears to be more difficult because of its nonlinear dependence on the stress history. *Robin* [1973] suggested that

$$\phi_1 = 1 - v_p \beta_s \frac{\partial v_p}{\partial p}, \tag{27}$$

where v_p is the pore volume, β_s is the rock compressibility in fractured media, and $\partial v_p/\partial p$ is the rate of change in pore volume with applied hydrostatic pressure for a joint with no pore fluid.

Based on an experimental study, *Walsh* [1981] suggested that ϕ_1 varies between 0.5 and 1. In that work it was determined that $\phi_1 = 0.9$ for joints with polished surfaces and $\phi_1 = 0.56$ for a joint made from a tension fracture.

Kranz et al. [1979] expressed their results in a similar manner, proposing that ϕ_1 should be less than 1 for jointed rock, and ϕ_1 approximates 1 for whole rock. They pointed out that the stress dependence of ϕ_1 is a function of both surface roughness and ambient pressure.

To determine ϕ_1 and ϕ_2 in this research, *Suklie*'s [1969] proposal is extended for dual-porosity media. As a first approximation, the difference between the bulk modulus of the fractured rock and that of the rock without fractures is neglected. The volumetric strain can be expressed as

$$\theta = \frac{\sigma_{kk}}{3K} - \sum_{m=1}^{2} \frac{p_m}{K}\left[1 - (1 - n_m)\frac{K}{K_s}\right], \tag{28}$$

where n_m is the porosity of phase m. Note that the volumetric strain, $\theta = \varepsilon_{kk}$, yields

$$\phi_i = 1 - (1 - n_i)\frac{K}{K_s} \qquad i = 1, 2 \tag{29}$$

In general, $n_1 < n_2$; therefore $\phi_1 < \phi_2$. It is readily confirmed [*Kranz et al.*, 1979; *Walsh*, 1981] that ϕ increases with a decrease in fracturing.

Relative compressibility, ϕ_m^*, may be expressed as

$$\phi_m^* = \left(\frac{1 - n_m}{K_s} + \frac{n_m}{K_f}\right). \tag{30}$$

The variable k_m in (10) represents the permeabilities of the fractures and matrix for $m = 1$ and 2, respectively. To evaluate fracture permeability k_1, we assume an idealized, regularly spaced, fracture system (Figure 9). If the fracture opening is estimated either from direct measurements or through pressure/flow relationships, then the fracture permeability in the direction parallel to each fracture set may be calculated directly from parallel plate analogy [*Snow*, 1968; *Louis*, 1969] as follows:

$$k_1 = \frac{b^3}{12s}, \tag{31}$$

where b is the fracture opening and s is the fracture spacing. Fracture permeability may also be obtained from in situ measurements such as pumping tests, provided that the flux contribution from the matrix may be verified as minimal.

Matrix permeability, k_2, may be estimated if the hydraulic radius, d, of the capillaries or pores is known or can be estimated. A suitable capillary equation can be used to calculate the permeability [*Bear*, 1972] as

$$k_2 = \frac{n_2^3}{(1 - n_2)^2}\frac{d^2}{180}, \tag{32}$$

where n_2 is the matrix porosity, and d is the mean grain size or hydraulic radius. As an alternative, pumping tests may be conducted in the porous medium alone to yield values of the primary permeability, k_2.

It should be noted that the fracture and porous medium permeabilities described previously are initial values. Since fracture apertures and capillary diameters are influenced by stress changes, the initial magnitudes of permeability will be modified as the stress field varies.

The remaining term to be determined is ξ in (10). On the basis of dimensional analysis and the assumption of quasi-steady flow conditions, *Barenblatt et al.* [1960] defined that the rate of fluid mass transfer from the porous matrix blocks to the fractures is given as

$$\xi = \xi_0(k_2 S_s^2), \tag{33}$$

where ξ_0 is a leakage constant, k_2 is the matrix permeability, and S_s is the specific surface of the fractures, i.e., the surface area of fractures per unit volume of the porous medium. For three mutually orthogonal fracture sets, *Warren and Root* [1963] defined

$$\xi_0 S_s^2 = \frac{60}{s^2}, \tag{34}$$

3.3. *Physical Parametric Identification*

In *Biot*'s [1941] Navier (displacement type) formulation of a deformation-dependent flow system, the governing equations were established without referring explicitly to the

undrained and drained stages of loading, as considered in the stress-based method proposed by *Rice and Cleary* [1976].

In the stress-based method, the governing equation of the solid phase can be expressed as [*Cleary*, 1977]

$$Gu_{i,kk} + \frac{G}{1-2\nu} u_{k,ki} + \frac{3(\nu_u - \nu)}{B(1+\nu_u)(1-2\nu)} p_{,i} = 0, \tag{35}$$

where ν_u and ν are the undrained and drained Poisson ratios, respectively; B is Skempton's constant [*Skempton*, 1954] which is defined as the change in pore pressure per unit change in confining pressure under undrained conditions.

The governing equation in the fluid phase may be written as

$$-\frac{1}{\mu} kp_{,kk} = \frac{3(\nu_u - \nu)}{BE(1+\nu_u)} \left[\dot{\sigma}_{kk} - \frac{3}{B} \dot{p} \right]. \tag{36}$$

To modify (36) into a form similar to (7), we have

$$-\frac{1}{\mu} kp_{,kk} = \frac{3(\nu_u - \nu)}{B(1+\nu_u)(1-2\nu)} \dot{\varepsilon}_{kk} - \frac{9(\nu_u - \nu)}{B^2 E(1+\nu_u)} \dot{p}. \tag{37}$$

Due to identical unknowns in terms of the fluid phase in (7) for the displacement-based method and (37) for the stress-based method, the following relationships are readily obtained:

$$\phi = \frac{3(\nu_u - \nu)}{B(1+\nu_u)(1-2\nu)} \tag{38}$$

$$\phi^* = \frac{9(\nu_u - \nu)}{B^2 E(1+\nu_u)}. \tag{39}$$

The pressure ratio factor ϕ may be modified from (21) by substituting (22) to yield

$$\phi = \frac{E}{3(1-2\nu)} \left(\frac{1}{K} - \frac{1}{K_s} \right). \tag{40}$$

Comparing (38) with (40), the Skempton constant may be expressed as

$$B = \frac{9(\nu_u - \nu)}{E(1+\nu_u)} \left(\frac{1}{K} - \frac{1}{K_s} \right)^{-1}. \tag{41}$$

Noting (21), and for the case $K \ll K_s$, (41) collapses to (38) with $\phi = 1$.

The relative compressibility ϕ^* may be determined by (24) or (25). In addition, *Geertsma* [1957] suggested adding the influence of the compressibility of solid skeleton ($1/K$), that is,

$$\phi^* = \frac{n}{K_f} + \frac{1-n}{K_s} - \frac{K}{K_s^2}. \tag{42}$$

If Geertsma's interpretation of Biot's constant R is used, however, ϕ^* can be expressed by *Rice and Cleary* [1976] as

$$\phi^* = \frac{n}{K_f} - \frac{1+n}{K_s} + \frac{1}{K}. \tag{43}$$

In (43), it appears that the partial compressibility of the solid skeleton of porous media, due to the change in fluid pressure, is additionally considered.

In any case, if ϕ^* is kept as a selective parameter, the coefficient B can be derived from (39) as

$$B = \left(\frac{9(\nu_u - \nu)}{\phi^* E(1+\nu_u)} \right)^{1/2}. \tag{44}$$

Equating (41) and (44) with substitution of (22), and further letting

$$\psi = \frac{E}{9H^2\phi^*}, \tag{45}$$

undrained and drained Poisson ratios ν_u and ν may be explicitly expressed by the other parameters:

$$\nu_u = \frac{\nu + \psi}{1 - \psi}, \tag{46}$$

$$\nu = \nu_u - \psi(1 + \nu_u), \tag{47}$$

It is understood from (45) that $\psi \geq 0$; therefore $\nu_u \geq \nu$. If $\psi = 0$ and $\nu_u = \nu$, then $\phi = 0$ and the fluid flow is fully decoupled from the solid deformation. Since [*Rice and Cleary*, 1976] $1/2 \geq \nu_u \geq \nu$, the following relation exists: $0 \leq \psi \leq (1 - 2\nu)/3$. By substituting (46) into (44), Skempton's constant B may be represented by the following simple expression:

$$B = \frac{1}{H\phi^*}. \tag{48}$$

Skempton's constant B may be written out by substituting (22) and ϕ^* in (24) or (25), or (42) or (43) into (48). For example, substituting (43) and (22) into (48), gives

$$B = \left[\frac{1}{K} - \frac{1}{K_s} \right] \left[\frac{n}{K_f} - \frac{1+n}{K_s} + \frac{1}{K} \right]^{-1}. \tag{49}$$

When $K \ll K_s$, which is often the case for soil,

$$B = \left[1 + \frac{nK}{K_f} \right]^{-1}. \tag{50}$$

This is the identical form of B as proposed by *Skempton* [1954]. If, however, (25) is used for ϕ^* in (48), one has

$$B = \left[\frac{1}{K} - \frac{1}{K_s} \right] \left[\frac{n}{K_f} + \frac{1-n}{K_s} \right]^{-1}. \tag{51}$$

For the case $K_s \gg K$ and $K_s \gg 1$,

$$B = \frac{K_f}{nK}, \tag{52}$$

which appears the most simplified representation of B. This is the case in Skempton's theory where the compressibility of the fluid is far greater than that of the soil structure. There is no obvious constraint for B if (52) is used in contrast to (50) of Skempton's theory. The characteristic of unbounded B (not confined between 0 and 1) under certain circumstances was also reported by *Elsworth and Bai* [1992].

TABLE 1*a*. Parameters for Case 1

Layer	k_f/μ	k_m/μ	E	ν	K_n	s	K_{fluid}	n_f	n_m
floor	0.88×10^{-4}	0.22×10^{-5}	1×10^6	0.28	3×10^6	10	5×10^7	0.05	0.20
3	0.44×10^{-3}	0.23×10^{-4}	2×10^6	0.20	6×10^6	3	8×10^7	0.10	0.25
2	0.66×10^{-4}	0.33×10^{-5}	3×10^6	0.25	9×10^6	5	1×10^7	0.12	0.23
1	0.59×10^{-2}	0.73×10^{-4}	2×10^6	0.22	8×10^6	2	1×10^7	0.08	0.15

Since Skempton's constant B was obtained from the undrained test, from (7) in the initial undrained case,

$$\Delta p = -\frac{\phi}{\phi^*}\Delta\varepsilon_{kk}, \tag{53}$$

or through conversion between the total strain and total stress,

$$\Delta p = -\frac{\phi}{3\phi^* K}\Delta\sigma_{kk}. \tag{54}$$

With reference to *Skempton* [1954],

$$\Delta p = -\frac{B}{3}\Delta\sigma_{kk}. \tag{55}$$

Substituting ϕ in (21) into (54), it is easily shown that B in (55) gives the identical form as in (48). The generalization of Skempton's constant B by (48) is a useful tool in the physical identification of the deformation-dependent flow parameters.

4. Finite Element Discretization of the Dual-Porosity Model

A multiporosity medium of particular interest in reservoir engineering is naturally fractured rock mass. The normal assumption for the fractured medium is that it possesses two degrees of porosity and two degrees of permeability, as seen in the governing equations (8) and (10), where the fracture geometry has been implicitly expressed. In the following, a finite element formulation is presented while all key parameters defined previously are incorporated.

The effective stress law for a dual-porosity medium may be expressed as

$$\sigma_{ij}^e = \sigma_{ij} - \phi_m p_m \delta_{ij}, \tag{56}$$

where $m = 1$ is a subscript for the fractures and $m = 2$ is a subscript for the matrix, and ϕ_m is the pressure ratio factor for phase m.

Applying the effective stress law enables the stress-strain relationship to be written for a dual-porosity medium as

$$\partial\boldsymbol{\sigma} = \mathbf{D}\left(\partial\boldsymbol{\varepsilon} + \sum_{m=1}^{2} \mathbf{C}\mathbf{m}\phi_m \partial p_m\right), \tag{57}$$

where $\boldsymbol{\sigma}$ and $\boldsymbol{\varepsilon}$ are vectors of stress and strain, respectively; p_m is the fluid pressure for phase m, $\mathbf{C}$ is a compliance matrix, $\mathbf{D}$ is an elasticity matrix, and $\mathbf{m}$ is a one-dimensional vector. For two-dimensional problems, $\mathbf{m}^T = \{1 \quad 1 \quad 0\}$.

Invoking the principle of virtual work and applying the incremental equilibrium to the total stress state results in

$$\int_V \mathbf{B}^T \partial\boldsymbol{\sigma}\, dv - \partial\mathbf{f} = 0, \tag{58}$$

where $\mathbf{B}$ is the strain displacement matrix, $\mathbf{f}$ is a vector of applied boundary tractions, and the integration is completed over the domain, V.

Substitution of (57) into (58) enables the governing finite element discretization for the solid phase to be given as

$$\mathbf{K}_T \frac{d\mathbf{u}}{dt} + \mathbf{R}\frac{d\mathbf{p}}{dt} = \frac{d\mathbf{F}}{dt}, \tag{59}$$

where

$$\mathbf{K}_T = \int_V \mathbf{B}^T \mathbf{D}\mathbf{B}\, dV, \tag{60}$$

$$\mathbf{R} = \sum_{m=1}^{2} \int_V \mathbf{B}^T \mathbf{D}\mathbf{C}\,\mathbf{m}\phi_m \mathbf{N}\, dV, \tag{61}$$

$$\mathbf{F} = \int_S \mathbf{N}\mathbf{f}\, dS, \tag{62}$$

where $\mathbf{N}$ is a vector of shape functions and S is the domain surface on which surface traction f is applied.

Darcy's velocity can be defined as

TABLE 1*b*. Notation for Table 1*a*.

Parameter	Term	Unit	Conversion
k_f/μ	fracture permeability	feet^4 pound^{-1} yr^{-1}	6.15×10^{-5} m^4 MN^{-1} s^{-1}
k_m/μ	matrix permeability	feet^4 pound^{-1} yr^{-1}	6.15×10^{-5} m^4 MN^{-1} s^{-1}
E	Young's modulus	pounds per square foot (psf)	47.88 Pa
ν	Poisson ratio	...	...
K_n	fracture stiffness	psf/foot	157.1 Pa/m
s	fracture spacing	feet	0.3048 m
K_{fluid}	fluid bulk modulus	psf	47.88 Pa
n_f	fracture porosity	...	...
n_m	matrix porosity	...	...

$$\mathbf{v} = -\frac{k}{\mu}\nabla(\mathbf{p} + \gamma z), \tag{63}$$

where k is the permeability, z is the elevation of the control volume, and γ is the unit weight of the fluid. The principle of continuity of flow requires that the divergence of the flow velocity vector be equal to the rate of fluid accumulation per unit volume of space. This must include the sum of the change in the total volumetric strain, the change in the solid grain volume, and the fluid volume change due to pressure change. In addition, the volume change due to the fluid transfer from the matrix to the fractures or vice versa must also be included. Volume changes from all of these sources may be defined as

$$\nabla^T\mathbf{v} = \mathbf{m}^T\phi_m\frac{\partial\boldsymbol{\varepsilon}}{\partial t} - \phi_m^*\frac{\partial\mathbf{p}}{\partial t} \pm \xi(\Delta\mathbf{p}), \tag{64}$$

where ϕ_m^* is defined in (30) and $\Delta\mathbf{p}$ is the fluid pressure difference between the fracture and pore phases.

Substituting (63) into (64) and invoking the Galerkin finite element procedure yields

$$\mathbf{E}\mathbf{p} + \mathbf{L}\frac{\mathbf{u}}{dt} + \mathbf{M}\frac{d\mathbf{p}}{dt} = \mathbf{Q}^*\Delta\mathbf{p} + \mathbf{G}\mathbf{Z}, \tag{65}$$

where

$$\mathbf{E} = -\frac{1}{\mu}\int_V \nabla\mathbf{N}^T\mathbf{k}\nabla\mathbf{N}\,dV \tag{66a}$$

$$\mathbf{L} = \phi_m\int_V \mathbf{N}^T\mathbf{m}^T\mathbf{C}\,\mathbf{D}\mathbf{B}\,dV = \mathbf{R}^T \tag{66b}$$

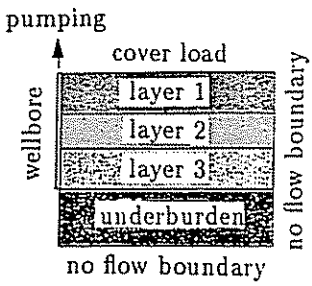

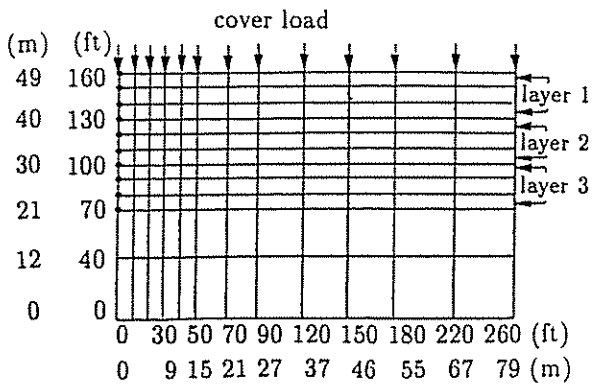

Fig. 10. Finite element layout for case study 1.

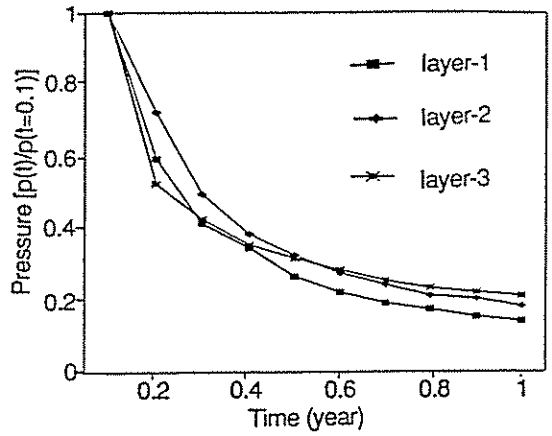

Fig. 11. Time-dependent pressure curves.

$$\mathbf{M} = -\phi_m^*\int_V \mathbf{N}^T\mathbf{N}\,dV \qquad \mathbf{Q}^* = \xi\int_V \mathbf{N}^T\mathbf{N}\,dV \tag{66c}$$

$$\mathbf{G} = \frac{1}{\mu}\int_V \nabla\mathbf{N}^T\mathbf{k}\nabla\mathbf{N}\,dV, \tag{66d}$$

where ξ has been defined by (33) and (34) and $\mathbf{k}$ is the permeability matrix.

Equations (59) and (65) completely define the finite element formulation of a dual-porosity problem. It is convenient to express these equations in a matrix form as

$$\begin{pmatrix}\mathbf{0} & \mathbf{0}\\ \mathbf{0} & \mathbf{E}\end{pmatrix}\begin{pmatrix}\mathbf{u}\\ \mathbf{p}\end{pmatrix} + \begin{pmatrix}\mathbf{K}_T & \mathbf{R}\\ \mathbf{L} & \mathbf{E}\end{pmatrix}\begin{pmatrix}\dot{\mathbf{u}}\\ \dot{\mathbf{p}}\end{pmatrix} = \begin{pmatrix}\dot{\mathbf{F}}\\ \mathbf{G}\mathbf{Z}\end{pmatrix} \pm \begin{pmatrix}\mathbf{0}\\ \mathbf{Q}^*\end{pmatrix}\begin{pmatrix}\mathbf{0}\\ \Delta\mathbf{p}\end{pmatrix}. \tag{67}$$

In comparison with the single-porosity formulation [*Ghaboussi and Wilson*, 1973], it is readily verified that when the fracture spacing implied in (57) is increased to infinity and parameters ϕ_1, ϕ_1^*, and ξ vanish, the dual-porosity model collapses to the single-porosity model.

The continuous time in (67) may be approximated by an implicit, finite difference time discretizing scheme:

$$\begin{pmatrix}\mathbf{K}_T & \mathbf{R}\\ \mathbf{L} & \Delta t\mathbf{E} + \mathbf{M}\end{pmatrix}\begin{pmatrix}\mathbf{u}\\ \mathbf{p}\end{pmatrix}^{t+1} = \begin{pmatrix}\mathbf{K}_T & \mathbf{R}\\ \mathbf{L} & \mathbf{E}\end{pmatrix}\begin{pmatrix}\mathbf{u}\\ \mathbf{p}\end{pmatrix}^{t} + \begin{pmatrix}\mathbf{F}\\ \Delta t\mathbf{G}\mathbf{Z}\end{pmatrix}^{t+1} + \begin{pmatrix}\mathbf{F}\\ \mathbf{0}\end{pmatrix}^{t} \pm \begin{pmatrix}\mathbf{0}\\ \Delta t\mathbf{Q}^*\end{pmatrix}\begin{pmatrix}\mathbf{0}\\ \Delta\mathbf{p}\end{pmatrix}^{t+1} \tag{68}$$

5. Quasi-Steady Flow Interaction Between Fractures and Matrix Blocks

As mentioned previously, the important difference between a single-porosity model and a dual-porosity model rests on the additional flow transfer mechanism in a dual-porosity formulation, representing the fluid interchange between the fracture and porous matrix phases as a result of the pressure differentiation between the two phases. Although a more rigorous transient flow system can be employed, for simplicity, only a quasi-steady flow system is used here. Following a mechanism proposed by *Barenblatt et al.* [1960] and simplified by *Warren and Root* [1963], fluid transfer rate may be evaluated by

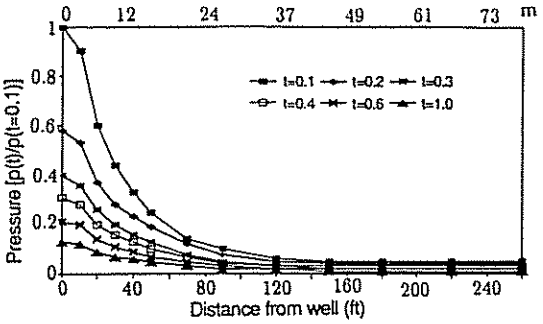

Fig. 12. Pressure versus distance at layer 3.

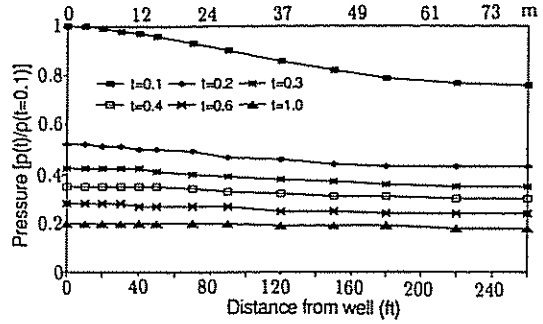

Fig. 14. Pressure versus distance at layer 1.

$$\xi = \frac{60}{s^2}\frac{k_2}{\mu}\Delta p \tag{69}$$

where k_2 is the matrix permeability and Δp is the pressure difference between the fracture phase and porous matrix.

6. Fracture Flow and Strata Deformation

The heterogeneous porous medium containing porosity within both fractures and pores may be idealized as a dual-porosity medium as discussed previously. For the case of a low-permeable rock and where the fracture flow dominates, the behavior of the porous media essentially reduces to that of an equivalent single-porosity formation. Neglecting turbulent flow and assuming that the primary flow is within the fracture network, the permeability of a set of parallel fractures of spacing s is given by (31), which expresses the permeability as a function of an initial fracture aperture. Since the aperture of the individual fractures will change with the solid body strain, the permeability of the strata will therefore be sensitive to the strata deformation as a result of petroleum production.

Assuming that the individual fractures are distinctly soft with respect to the porous medium, the deformation-modified permeability may be written as [*Elsworth*, 1989]

$$k = \frac{1}{12s}(b + s\Delta\varepsilon)^3, \tag{70}$$

where $\Delta\varepsilon$ is the body strain perpendicular to the fracture set.

When the compliance of the elastic matrix approaches that of the fracture, the modulus of the matrix must be included in the evaluation of the permeability enhancement. Total displacements are the sum of the elastic displacements in the matrix and across the fracture (shear displacement and dilation are neglected). As a result, the modified permeability of a single fracture set that incorporates solid deformation may be calculated using

$$k = \frac{b^3}{12s}\left[1 + \Delta\varepsilon\left(\frac{K_n b}{E} + \frac{b}{s}\right)^{-1}\right]^3. \tag{71}$$

A comparison between (31) and (71) indicates that the effect of induced strains is controlled by the dimensionless terms $(K_n b)/E$ and b/s. Permeability will not be influenced when these terms are individually, or collectively, very large.

7. Model Application

In the past the deformation-dependent flow model was rarely used in the reservoir simulation, due primarily to the added complication of the coupled deformation flow system, and due further to the difficulty in determining the multitude of nonlinear parameters that describe the system. An attempt is made in the following to apply the dual-porosity/dual-permeability model described previously to two simple, hypothetical case studies. The objective of this preliminary investigation is to delineate the influence on the fluid pressure distribution contributed by the change in external loading configuration and deformation magnitudes. For generality, dimensionless analysis prevails. As a result, the excess pressure and strain as well as their signs are presented in a relative fashion. For simplicity, a single fluid component such as oil in the fractured reservoir is assumed.

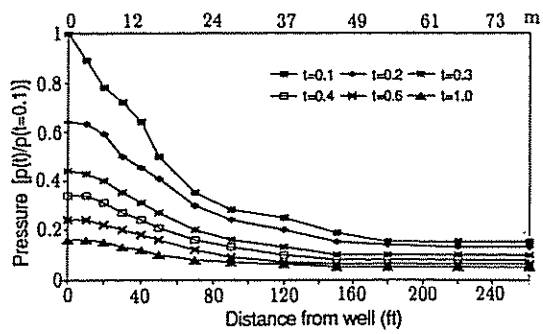

Fig. 13. Pressure versus distance at layer 2.

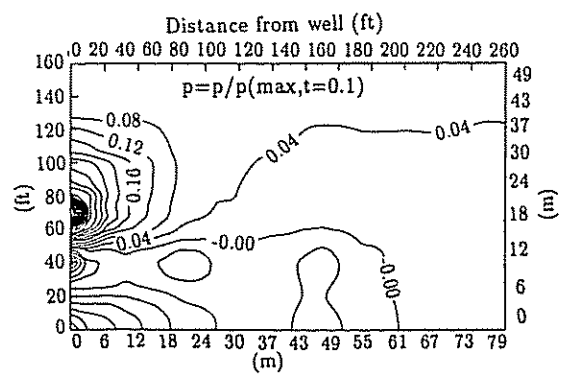

Fig. 15. Pressure distribution at $t = 0.1$ year (case study 1).

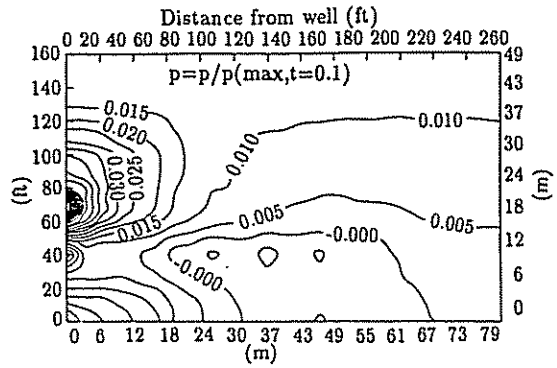

Fig. 16. Pressure distribution at t = 1 year (case study 1).

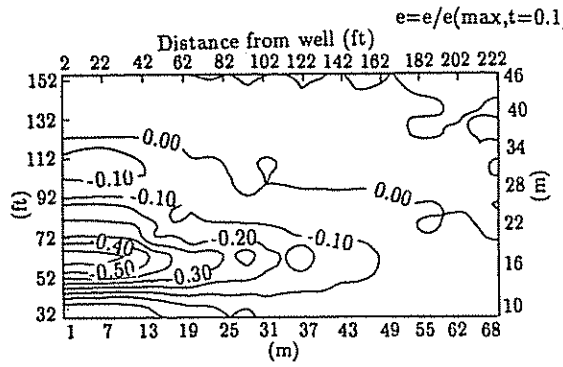

Fig. 18. Strain distribution at t = 1 year (case study 1).

7.1. *Case Study 1*

A flat-lying reservoir is located at a depth of 6000 feet (1829 m) and contains three layers distinguished by the material properties listed in Table 1. The specific weight of overburden is 2.67. A gravitational cover load of 1×10^6 pounds per square foot (47.88 MPa) is assumed to act on the top of the reservoir. The oil-saturated reservoir (all three layers) is being produced at a constant rate of 500 feet^3 per day (1.64×10^{-4} m^3/s) through a fully penetrating well. It is assumed that no gas mixture is found in the oil, and no water drive mechanism is to be considered. No-flow conditions are assumed, both at the lateral boundary and at a distance of 70 feet (21.3 m) from the bottom layer of the reservoir. The oil flows outward from the well under initial fluid pressure.

As a result of symmetry, only one half of the reservoir in the lateral direction needs to be simulated in the finite element model (Figure 10). The specific flow rate is designated at the nodes along the centerline of the reservoir, as an approximation of a planar source. In expectation of more dramatic changes in the pressure and deformation near the well bore, a denser mesh is placed in the vicinity of the well. Soft underburden is assumed beneath the reservoir (Table 1). The porous media are represented by a dual-porosity system where an orthogonal fracture network of regular spacing intervenes between adjacent matrix blocks.

The dimensionless pressure depletion curves are shown in Figure 11 for the locations of (10 feet, 80 feet), (10 feet, 110 feet) and (10 feet, 140 feet) ((3 m, 24.4 m), (3 m, 33.5 m) and (3 m, 42.7 m)), respectively. For layer 3, the pressure declines faster initially and more slowly at the later stage. The opposite is true for layer 2. For each individual layer, the time-dependent pressure-distance curves are given in Figures 12–14. The fastest decline of fluid pressure is observed in layer 3, in contrast to the slowest observed in layer 1, indicating the significant influence of reservoir compression and higher compliance in the underburden.

The pressure contours at t = 0.1 year and t = 1 year are shown in Figures 15 and 16. The higher pressure magnitudes are associated with the location of the well and occur in the vicinity of the interface between the reservoir and the underburden. In view of the change in pressure magnitudes, the time period within 1 year after the initial oil production is identified as the most prominent. Figures 17 and 18 are the strain distribution at t = 0.1 year and t = 1 year, respectively. In particular, at a later stage, higher strain magnitudes occur in the underburden region.

In a dual-porosity or fractured porous medium, the period of transient interactive flow between the fracture phase and matrix phase can be relatively short. Figure 19 represents the time-dependent pressure variation in the fracture phase and matrix phase at different periods. It is seen that the interactive flow occurs before t = 0.2 year. The fluid interchange between the fracture phase and the matrix phase slows the rate of fluid transport in a fractured porous formation.

7.2. *Case Study 2*

The previous case represents the pressure variation in a cross-sectional view of the reservoir subjected to the cover load. In an areal model, a reservoir may be subjected to excessive tectonic stress as indicated in Figure 20, which

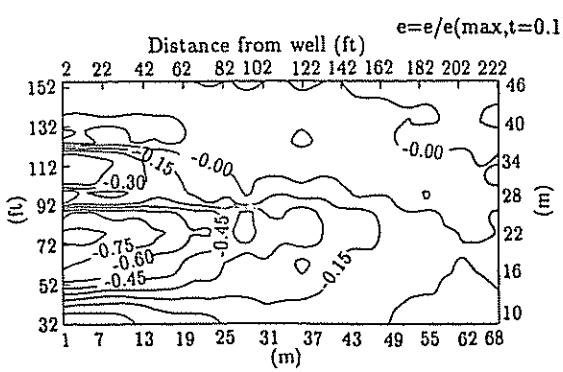

Fig. 17. Strain distribution at t = 0.1 year (case study 1).

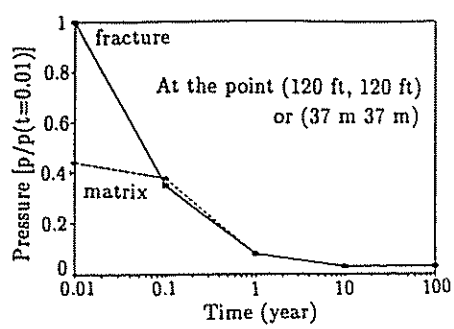

Fig. 19. Pressure depletion in fracture and matrix.

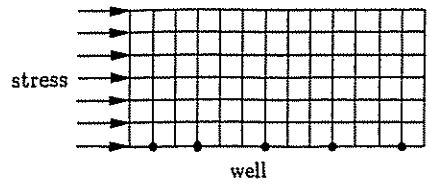

Fig. 20. Finite element layout for case study 2.

also shows the finite element mesh layout in a simulated half-reservoir section with five production wells. The boundary stress acting on the left border of the reservoir is instantaneously applied. The material constants of the reservoir are identical to those of layer 2 given in Table 1. Figure 21 represents the changes of the relative pressure distribution after 0.1 years of production. No obvious pressure variation during this period is observed. If relatively large magnitudes of stress are applied (Figure 22), however, the pressure distribution will be substantially different from the previous cases due to a more significant deformation effect. The greater variation of the pressure is demonstrated at the locations close to the stressed boundaries.

8. CONCLUSIONS

This paper has systematically introduced several conceptual deformation-dependent flow models utilizing concepts of multiporosity and multipermeability that may be suitable for the characterization of a variety of formation types. A unified multiporosity/multipermeability formulation has been proposed, which represents a generalization of the porosity or permeability-oriented models of various degrees. Deviating from the traditional porosity-oriented model conceptualization, permeability stands out as one of the critical factors in rationalizing reservoir behavior. The practical implication of these models is aimed at providing additional and more flexible tools in matching the geological variation inherent in real reservoirs.

In a parametric study, some key constants are identified and are expressed in terms of experimentally measurable coefficients. A simple relationship has been derived to express Skempton's constant B using only Biot's constant H and relative compressibility ϕ^*. This relationship signifies a successful parametric communication between the displacement-based [*Biot*, 1941] and the stress-based [*Rice and Cleary*, 1976] methods in the description of deformation-dependent flow system.

An alternative finite element approximation to the dual-porosity/dual-permeability formulation is introduced. Although the formulation is based on the theory of mixtures

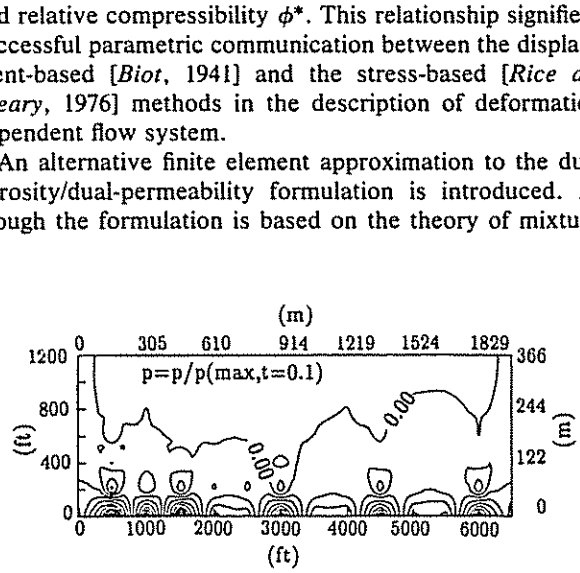

Fig. 21. Pressure distribution at t = 0.1 year (case study 2).

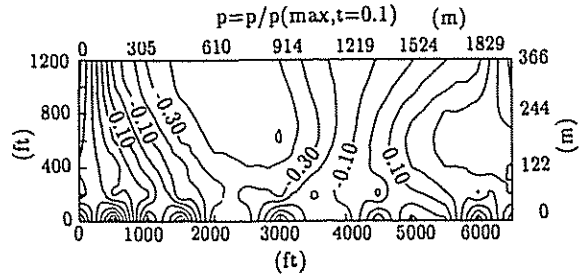

Fig. 22. Pressure distribution at t = 0.1 year (case study 2) for relatively large magnitudes of stress.

where the fracture phase and porous matrix phase are represented by two overlapping continua, the deformation-dependent fracture flow mechanisms is readily coupled where the rock matrix possesses low permeability and flow is dominant in the fractures.

A preliminary study of reservoir simulation using the theory of deformation-dependent flow identifies the strong coupling between fluid flow and solid deformation. Variation in material constitutive properties may result in a different change in the pressure and strain profiles. Neglecting an important factor, such as strata deformation, may therefore introduce a significant error in the reservoir analysis.

REFERENCES

Abdassah, D., and I. Ershaghi, Triple-porosity system for representing naturally fractured reservoirs, *SPE Form. Eval.*, *1*, 113–127, 1986.

Aguilera, R., *Naturally Fractured Reservoirs*, Petroleum, Tulsa, Okla., 1980.

Aifantis, E. C., Introducing a multi-porous medium, *Dev. Mech.*, *9*, 209–211, 1977.

Aifantis, E. C., On the problem of diffusion in solids, *Acta Mech.*, *37*, 265–296, 1980.

Barenblatt, G. I., I. P. Zheltov, and N. Kochina, Basic concepts in the theory of seepage of homogeneous liquids in fissured rocks, *Prikl. Mat. Mekh.*, *24*(5), 852–864, 1960.

Bear, J., *Dynamics of Fluids in Porous Media*, 764 pp., Elsevier, New York, 1972.

Biot, M. A., General theory of three-dimensional consolidation, *J. Appl. Phys.*, *12*, 155–164, 1941.

Chen, C. C., K. Serra, A. C. Reynolds, and R. Raghavan, Pressure transient analysis methods for bounded naturally fractured reservoirs, *SPEJ Soc. Pet. Eng. J.*, *25*, 451–464, 1985.

Cleary, M. P., Fundamental solutions for a fluid-saturated porous solid, *Int. J. Solids Struct.*, *13*, 785–806, 1977.

deSwaan-O., A., Analytical solutions for determining naturally fractured reservoir properties by well testing, *Soc. Pet. Eng. J.*, *16*, 117–122, 1976.

Detournay, E., and A. H.-D. Cheng, Poroelastic response of a borehole in a non-hydrostatic stress field, *Int. J. Rock Mech. Min. Sci. Geomech. Abstr.*, *25*(3), 171–182, 1988.

Duguid, J. O., and P. C. Y. Lee, Flow in fractured porous media, *Water Resour. Res.*, *13*(3), 558–566, 1977.

Elsworth, D., Thermal permeability enhancement of blocky rocks: One-dimensional flows, *Int. J. Rock Mech. Min. Sci. Geomech. Abstr.*, *26*(3/4), 329–339, 1989.

Elsworth, D., and M. Bai, Coupled flow-deformation response of dual porosity media, *J. Geotech. Eng.*, *118*(1), 107–124, 1992.

Geertsma, J., The effect of fluid pressure decline on volumetric changes of porous rocks, *Trans. Am. Inst. Min. Metall. Pet. Eng.*, *210*, 331–340, 1957.

Ghaboussi, J., and E. L. Wilson, Flow of compressible fluid in porous elastic media, *Int. J. Numer. Methods Eng.*, *5*, 419–442, 1973.

Huyakorn, P. S., and G. Pinder, *Computational Methods in Subsurface Flow*, Academic, San Diego, Calif., 1983.

Kazemi, H., Pressure transient analysis of naturally fractured reservoirs with uniform fracture distribution, *Soc. Pet. Eng. J.*, *9*, 451–461, 1969.

Kranz, R. L., A. D. Frankel, T. Engelder, and C. H. Scholz, The permeability of whole and jointed Barre granite, *Int. J. Rock Mech. Min. Sci. Geomech. Abstr.*, *16*(3), 225–234, 1979.

Kucuk, F., and W. K. Sawyer, Transient flow in naturally fractured reservoirs and its application to Devonian gas shales, paper SPE 9397 presented at the 1980 SPE Annual Technical Conference and Exhibition, *Soc. of Pet. Eng.*, Dallas, Tex., Sept. 21–24, 1980.

Lewis, R. W., and B. A. Schrefler, *The Finite Element Method in the Deformation and Consolidation of Porous Media*, 344 pp., John Wiley, New York, 1987.

Liggett, J. A., and P. L. F. Liu, *The Boundary Integral Equation Method for Porous Media Flow*, Allen and Unwin, Winchester, Mass., 1983.

Louis, C., Groundwater flow in rock masses and its influence on stability, *Rock Mech. Res. Rep.*, *10*, Imp. Coll., London, 1969.

Najurieta, H. L., A theory for pressure transient analysis in naturally fractured reservoirs, *JPT J. Pet. Technol.*, *32*, 1241–1250, 1980.

Nur, A., and J. D. Byerlee, An exact effective stress law for elastic deformation of rock with fluids, *J. Geophys. Res.*, *76*(26), 6414–6419, 1971.

Rice, J. R., and M. P. Cleary, Some basic stress-diffusion solutions for fluid-saturated elastic porous media with compressible constituents, *Rev. Geophys.*, *14*, 227–241, 1976.

Robin, P. Y. F., Note on effective pressure, *J. Geophys. Res.*, *78*(14), 2434–2437, 1973.

Simon, B. R., O. C. Zienkiewicz, and D. R. Paul, An analytical solution for the transient response of saturated porous elastic solids, *Int. J. Numer. Anal. Methods Geomech.*, *8*, 381–398, 1984.

Skempton, A. W., The pore pressure coefficients A and B, *Geotechnique*, *4*, 143–147, 1954.

Skempton, A. W., Effective stress in solid, concrete and rock, *Pore Pressure and Suction in Soils*, Butterworths, London, 1960.

Snow, D. T., Rock fracture spacings, openings, and porosities, *J. Soil Mech. Found. Div. Am. Soc. Civ. Eng.*, *94*, 73–91, 1968.

Suklie, L., *Rheological Aspects of Soil Mechanics*, John Wiley, New York, 1969.

Terzaghi, K., *Theoretical Soil Mechanics*, John Wiley, New York, 1943.

Verruijt, A., An elastic storage of aquifers, in *Flow Through Porous Media*, pp. 331–376, Academic, San Diego, Calif., 1969.

Walsh, J. B., Effect of pore pressure and confining pressure on fracture permeability, *Int. J. Rock Mech. Min. Sci. Geomech. Abstr.*, *18*(3), 429–435, 1981.

Warren, J. E., and P. J. Root, The behavior of naturally fractured reservoirs, *Soc. Pet. Eng. J.*, *3*, 245–255, 1963.

Zienkiewicz, O. C., C. Humpheson, and R. W. Lewis, A unified approach to soil mechanics problems, in *Finite Element in Geomechanics*, edited by G. Gudehus, pp. 151–177, John Wiley, New York, 1977.

M. Bai and J.-C. Roegiers, University of Oklahoma, Norman, OK 73019-0628.

D. Elsworth, Pennsylvania State University, University Park, PA 16802.

(Received January 13, 1992;
revised November 10, 1992;
accepted November 18, 1992.)